JOURNAL OF APPLIED ELECTROCHEMISTRY 9 (1979) 161–169

Influence of lead and thallium underpotential adsorbates at silver single crystal surfaces on different redox reactions

C. MAYER*, K. JÜTTNER, W. J. LORENZ

Institute of Physical Chemistry and Electrochemistry, University of Karlsruhe, Germany

Received 6 March 1978

The influence of underpotential Pb- and Tl-adsorbates at rotating disc silver single crystal surfaces (1 1 1), (1 0 0), and (1 1 0) on the kinetics of 'outer-sphere' and 'inner-sphere' redox reactions was studied in 0·5 M $NaClO_4$ and 0·5 M Na_2SO_4 solutions ($2 < pH < 4$) containing Fe^{3+}, Ce^{4+} or NO_3^- ions. While the reduction of Fe^{3+} and Ce^{4+} under limiting diffusion conditions was not affected by the metal adsorbates, a strong inhibition effect correlated to the degree of Pb- or Tl-adsorbate coverages was observed in the case of the reduction process in the presence of NO_3^- ions. The results are interpreted in terms of a strong chemical interaction between the reactant or a reaction intermediate and the silver substrate, taking into account the previously proposed superlattice structures of the metal adsorbates, depending on the orientation of the silver single crystal surfaces and on the underpotential range.

1. Introduction

The underpotential deposition of lead and thallium on silver (1 1 1), (1 0 0), and (1 1 0) oriented single crystal surfaces has been studied extensively with respect to their thermodynamic and kinetic properties [1–17].

In the system Ag (1 1 1)/Pb^{2+} the experimental saturation coverage values, Γ_s, correspond to the formation of one close-packed Pb-monolayer Ag (1 1 1)–3(2 x 2)Pb, [3–8, 12–16]. However, in the system Ag(1 1 1)/Tl^+ two close-packed Tl-monolayers are formed [3–6, 9–15]. In the case of incomplete formation of the first layer on the Ag(1 1 1) substrate, a slow structural transformation has been observed starting presumably from adsorbate superlattices of lower density, e.g. the honeycomb structure Ag (1 1 1)–2(2 x 2) Pb or Tl [7, 9, 10]. From the slightly but significantly different Γ_s-values, and the different peak structures of the voltammograms as well as from the different shapes of the equilibrium isotherms depending on the substrate orientation, it has been concluded that the saturation coverages on Ag (1 0 0) and Ag (1 1 0) faces are better explained by assuming two layers of $c(2 \times 2)$ Pb and three layers of $c(2 \times 2)$ Tl superlattice structures [5–7, 9].

Kinetic studies in the systems Ag $(h\,k\,l)$/Pb^{2+} and Ag $(h\,k\,l)$/Tl^+ have shown that the adsorption processes are controlled by charge transfer and/or bulk diffusion [3, 4, 10]. The dominance of a first-order phase transformation, i.e. two-dimensional nucleation and growth [11–15], could not be confirmed [3, 4, 10].

The true state of charge of the adsorbed particles is not revealed by electrochemical charge and coverage measurements. The electrosorption valency $\gamma = F^{-1}(\partial q/\partial \Gamma)_E$ merely describes the interdependence of metal and non-metal adsorption processes. In the systems Ag $(h\,k\,l)$/Pb^{2+}, ClO_4^-, and Ag $(h\,k\,l)$/Tl^+, ClO_4^- or SO_4^{2-}, ideal charge-coverage stoichiometry $\gamma = z$ for Pb and Tl (where z is the metal ion charge number) has been found, ruling out any non-metal cosorption phenomena [7–9]. The charge distribution in the adsorption state and the distance between the adsorbed particles depend on the vertical interaction adsorbate–substrate and the lateral interaction adsorbate–adsorbate. From thermodynamic data, a strong lateral interaction in both systems

* Permanent address: Departamento de Ciencias Exactas, Universidad Nacional del Sur, Bahia Blanca, Argentina.

can be derived [3–5, 7–16] indicating a highly discharged state of the adsorbate. Moreover, a correlation between thermodynamic data and the difference of electronegativity between substrate and adsorbate supports the presumption of a highly discharged metal adsorbate in the underpotential range [17, 18]. Since $\Delta\chi = |\chi_s - \chi_{ad}| < 0{\cdot}3$ and $\gamma/z = 1$ in both systems, a covalent bond formation between the substrate and the adsorbate can be assumed according to Pauling [17–19]. Therefore, Pb- and Tl-submonolayers on silver substrates might be considered as covalent bound catalysts or inhibitors for electrochemical reactions.

Generally, the effects of surface layers on the kinetics of electrochemical processes arise from the following phenomena [18]:

(a) a chemical interaction between the reactant, or an intermediate and a covalent bound adsorbate,

(b) a geometrical blocking effect of the metal adsorbate especially at active sites of the substrate surface,

(c) an electrostatic interaction between the reactant or an intermediate and a charged adsorbate,

(d) electronic effects in the case of thicker layers with low electronic conductivity.

According to the above-mentioned properties of the Pb- and Tl-adsorbates it is clear that only points (a) and (b) have to be taken into account.

The kinetics of outer-sphere electron charge transfer reactions, which take place at the outer Helmholtz plane, should not be influenced markedly by metal adsorbates. In agreement, the rates of the redox reactions Fe^{2+}/Fe^{3+} and Ti^{3+}/Ti^{4+} on Au and Pt electrodes were only slightly changed by Ag-, Pb-, Cd-, Bi-, Tl-, Cu-, Se-, and Te-layers [20–22].

On the contrary, strong chemical interactions should be observed in the case of inner-sphere electron charge transfer reactions which involve the formation or breaking of chemical bonds (electrosorption) of reactants or intermediates or, in the case of metal ion charge transfer processes. Indeed, this expectation had been partly confirmed by a series of papers dealing with the catalytic effect of metal adsorbates on different organic redox processes [23–30] as well as on the oxygen reduction [31] and the hydrogen evolution reactions [32–36].

All the previous work was carried out on polycrystalline substrates, and thus ignored the specific influence of the metal adsorbate structure in the underpotential range. The aim of this work is to investigate the influence of well-defined Pb- and Tl-adsorbates at silver single crystal surfaces on redox processes such as the reduction of Fe^{3+}, Ce^{4+}, and NO_3^- ions.

The redox reactions

$$Fe^{2+} \rightleftharpoons Fe^{3+} + e^-$$

and

$$Ce^{3+} \rightleftharpoons Ce^{4+} + e^-$$

are simple outer-sphere electron charge transfer processes [37–42].

However, the reduction mechanism of NO_3^- is very complicated and has not yet been completely elucidated [37, 43]. At platinum electrodes, in strong acid solutions containing NO_2^- and a high concentration of NO_3^- ions, a rate determining heterogeneous chemical reaction

$$H^+ + HNO_2 \rightleftharpoons NO^+ + H_2O \qquad (1)$$

followed by the fast chemical steps

$$NO^+ + NO_3^- \rightleftharpoons N_2O_4 \qquad (2)$$

$$N_2O_4 \rightleftharpoons 2\,NO_2 \qquad (3)$$

and a slow charge transfer process

$$2(H^+ + NO_2 + e^- \rightleftharpoons HNO_2) \qquad (4)$$

has been assumed [37, 43]. Reaction 1 causes a cathodic limiting current density which is independent of stirring. Reaction 1 followed by the electrochemical step

$$2(NO^+ + e^- \rightleftharpoons NO) \qquad (5)$$

and an autocatalytic reaction

$$2NO + H^+ + NO_3^- + H_2O \rightleftharpoons 3HNO_2 \qquad (6)$$

was proposed by other authors [44–46]. The adsorption of reaction intermediates at the electrode surface was also taken into consideration [43, 47].

In weaker acid solutions a primary hydrogen evolution step has been assumed [43].

$$H^+ + e^- \rightleftharpoons H_{ads} \qquad (7)$$

$$HNO_3 + 2H_{ads} \rightleftharpoons HNO_2 + H_2O \qquad (8)$$

From differential capacitance–potential measurements in the system Ag (1 1 1) and Ag (1 0 0)/x M

$NaNO_3 (10^{-3} < x < 10^{-2})$ it was concluded that an adsorption of NO_3^- ions takes place at the Ag(1 0 0) face only [48]. In the presence of 0·05 M Na_2SO_4 a limiting current density on Ag (1 0 0) has been observed which was attributed to the reduction of NO_3^- ions. Consequently, the reduction of NO_3^- seems to be an inner-sphere redox reaction.

2. Experimental

Cyclic voltammetric measurements were carried out on silver single crystal* surfaces of the orientations (1 1 1), (1 0 0) and (1 1 0) using the rotating disc technique. The voltage sweep rate was held constant $|dE/dt| = 10\,mV\,s^{-1}$.

The experimental details such as cell device, pretreatment of the single crystal surfaces and the electronic equipment used have been reported elsewhere [4, 6]. Electrolyte solutions were prepared from suprapure† or p.a.† grade reagents and bidistilled water. The solutions were deaerated by purified nitrogen ($O_2 < 2$ ppm). The geometric areas of the silver single crystal surfaces were about 0·75 cm^2. A $Hg/Hg_2SO_4, Na_2SO_4$ (satd) electrode served as a reference electrode. All potentials given in this paper are referred to the NHE. The experiments were carried out at $T = 298$ K.

To start with, cyclic voltammograms in the systems Ag $(h\,k\,l)/Pb^{2+}$ and Ag $(h\,k\,l)/Tl^+$ free of redox couples were recorded in order to verify the characteristic peak structures as a criterion for the quality of surface preparation. The reducible substances were added after attaining a reproducible voltammogram.

3. Results

The charge transfer controlled Fe^{3+}-reduction cannot be investigated in the system Ag $(h\,k\,l)/x$ M $H^+ + y$ M Fe^{3+} $(10^{-4} < y < 10^{-2})$ since at potentials $E_H < 500$ mV this reaction is bulk diffusion controlled [42] and at more positive potentials the anodic oxidation of the silver surface occurs. On the other hand, the underpotential

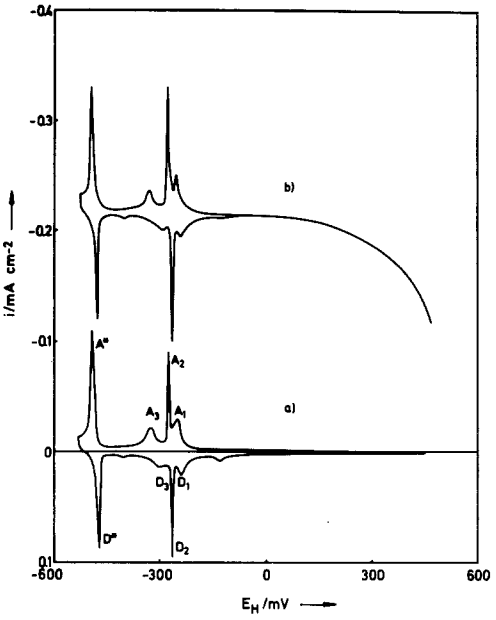

Fig. 1. System: Ag (1 1 1)/0·5 M $Na_2SO_4 + 10^{-3}$ M $HClO_4 + 7 \times 10^{-4}$ M $Tl_2SO_4 + y$ M $Fe_2(SO_4)_3$. (a) $y = 0$, (b) $y = 6 \times 10^{-4}$; $T = 298$ K, $|dE/dt| = 10\,mV\,s^{-1}$.

range‡ of Pb- and Tl-adsorption on Ag $(h\,k\,l)$ is situated at more negative potentials than the potential region of the charge transfer controlled Fe^{3+}-reduction. Therefore, only a geometrical blocking effect of adsorbed Pb or Tl on the bulk diffusion controlled Fe^{3+}-reduction should be detectable. However, such a blocking effect seems to be improbable in the case of an electron conducting metal adsorbate and an outer-sphere electron charge transfer reaction under limiting diffusion conditions.

This prediction was confirmed experimentally as can be seen from Fig. 1. The cyclic voltammogram in the presence of Tl^+ and Fe^{3+} only represents a simple superposition of both the Tl-adsorption and desorption on the Ag (1 1 1) substrate characterized by the sorption peaks A_1–A^* and D_1–D^* and the limiting diffusion current density of the Fe^{3+}-reduction. The same results were obtained in the cases of Ag (1 0 0) and Ag (1 1 0) substrate orientations, as well as for Pb instead of Tl-adsorption. Similar behaviour was found in the case of Ce^{4+}-ion reduction.

‡ The underpotential range is defined by $\Delta E = E - E_{Me/Me^{z+}}$, where $E_{Me/Me^{z+}}$ is the equilibrium potential given by the Nernst equation for Pb/Pb^{2+} and Tl/Tl^+, respectively. The ΔE values amount to about 200 mV and 400 mV for Pb and Tl adsorption, respectively [3–16].

* Materials Research.
† Merck.

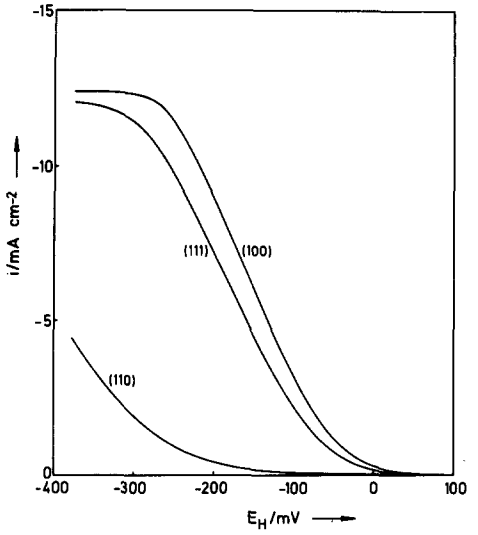

Fig. 2. System: Ag $(h\,k\,l)$/0·5 M $NaClO_4$ + 5 × 10^{-3} M $HClO_4$ + 0·1 M $NaNO_3$. pH = 2·4, T = 298 K, $|dE/dt|$ = 10 mV s^{-1}; rotation frequency 25 Hz.

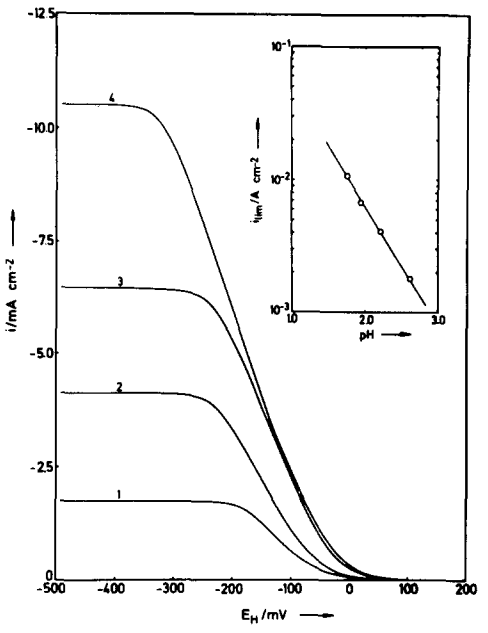

Fig. 4. System: Ag (1 0 0)/0·5 M $NaClO_4$ + x M $HClO_4$ + 0·1 M $NaNO_3$. pH = 2·61 (1), 2·22 (2), 1·94 (3), 1·74 (4); T = 298 K, $|dE/dt|$ = 10 mV s^{-1}; rotation frequency 25 Hz.

The present investigations concerning NO_3^--ion reduction were carried out in the systems

$$\text{Ag}\,(h\,k\,l)/0{\cdot}5\text{ M }NaClO_4 + 0{\cdot}1\text{ M }NaNO_3 + x\text{ M }HClO_4 + y\text{ M }Pb(ClO_4)_2 \qquad \text{(I)}$$

$$\text{Ag}\,(h\,k\,l)/0{\cdot}5\text{ M }Na_2SO_4 + 0{\cdot}1\text{ M }NaNO_3 + x\text{ M }HClO_4 + y\text{ M }Tl_2SO_4 \qquad \text{(II)}$$

in the range pH 2–4.

Figs. 2 and 3 show current density–potential curves in both systems, free of lead and thallium ions. In both cases, the charge transfer controlled part of the polarization curves depends strongly on the orientation of the silver substrate and is shifted towards more negative potentials in the sequence Ag (1 0 0), Ag (1 1 1), and Ag (1 1 0). The

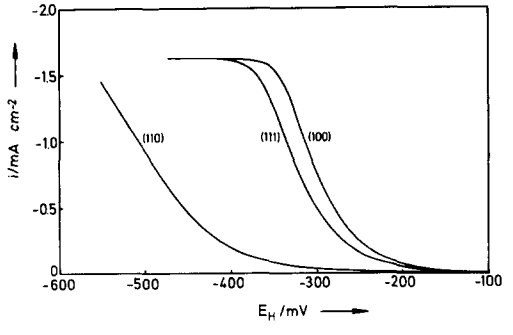

Fig. 3. System: Ag $(h\,k\,l)$/0·5 M Na_2SO_4 + 10^{-3} M $HClO_4$ + 0·1 M $NaNO_3$; pH = 3·7, T = 298 K, $|dE/dt|$ = 10 mV s^{-1}; rotation frequency 25 Hz.

shift amounts to about 20 mV between Ag (1 0 0) and Ag (1 1 1) and about 200 mV between Ag (1 1 1) and Ag (1 1 0), respectively.

The limiting current densities are independent of the substrate orientation (Figs. 2 and 3) and of the NO_3^- ion bulk concentration. However, they strongly depend on the pH-value of the electrolyte as can be seen from Fig. 4 and by comparing Figs. 2 and 3. A linear relation between $\log i_{lim}$ and pH with a slope of $(\partial \log i_{lim}/\partial\,\text{pH})_{a_i \neq a_{H^+}} \simeq 1$ is observed. Furthermore, the limiting current densities are functions of the angular velocity ω of the rotating disc as shown in Figs. 5 and 6. The linearity between i_{lim} and $\omega^{1/2}$ indicates a rate-determining bulk diffusion process. The experimental i_{lim} values are about one order of magnitude lower than would be expected for NO_3^- diffusion. On the other hand, their observed pH-dependence as well as the calculated mutual diffusion coefficients of about $D_i = 6 \times 10^{-5}$ $cm^{-2}\,s^{-1}$ in system I and $D_i = 3.6 \times 10^{-5}$ $cm^{-2}\,s^{-1}$ in system II indicate a dominant transport of protons [49]. In contrast to this, NO_2^- ions could be detected analytically in the electrolyte solution after extended polarization.

Cyclic voltammograms in the presence of lead

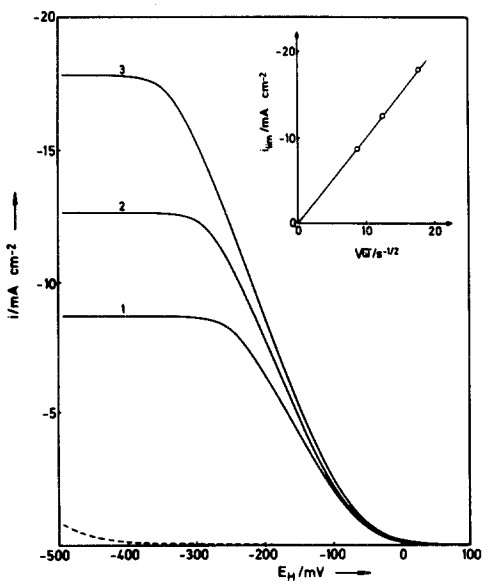

Fig. 5. System: Ag (1 0 0)/0·5 M $NaClO_4$ + 5 × 10^{-3} M $HClO_4$ + 0·1 M $NaNO_3$. $|dE/dt| = 10\ mV\ s^{-1}$; (——) rotation frequency = 12·5 Hz (1), 25 Hz (2), 50 Hz (3); (- - - -) without $NaNO_3$, rotation frequency 25 Hz, $T = 298$ K.

ions in system I are given in Fig. 7 for Ag (1 1 1) and in Fig. 8 for Ag (1 0 0) surfaces. The current density–potential curves in the absence of NO_3^- ions show the well-known peak structure of the underpotential lead deposition depending on the

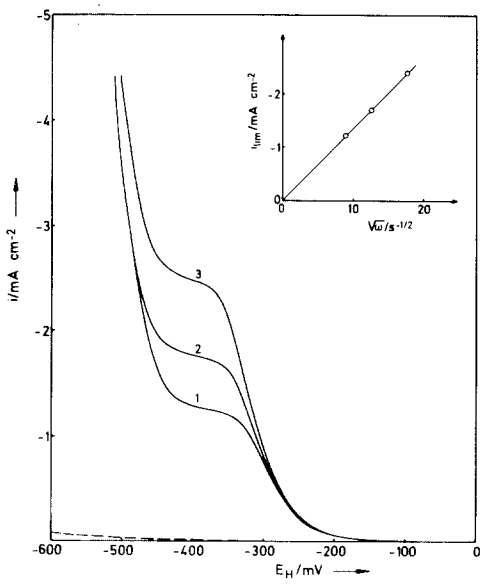

Fig. 6. System: Ag (1 0 0)/0·5 M Na_2SO_4 + 10^{-3} M $HClO_4$ + 0·1 M $NaNO_3$. $|dE/dt| = 10\ mV\ s^{-1}$, $T = 298$ K; (——) rotation frequency = 12·5 Hz (1), 25 Hz (2), 50 Hz (3); (- - - -) without $NaNO_3$, rotation frequency 25 Hz.

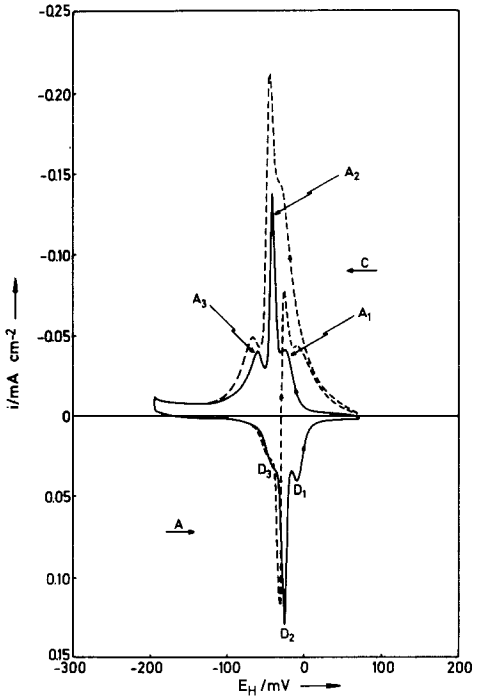

Fig. 7. System: Ag (1 1 1)/0·5 M $NaClO_4$ + 5 × 10^{-3} M $HClO_4$ + 5 × 10^{-4} M $Pb(ClO_4)_2$ + y M $NaNO_3$; (——) $y = 0$; (- - - -) $y = 0{\cdot}1$; $T = 298$ K, $|dE/dt| = 10\ mV\ s^{-1}$, rotation frequency 25 Hz.

substrate orientation [4, 5, 8, 12–16]. It can be seen that the reduction process occurring in the presence of NO_3^- ions is strongly influenced by the underpotential lead deposition.

On the Ag (1 1 1) face, the reduction current decreases at the lead potential peak A_2 and vanishes after completing the Pb-monolayer in peak A_3 (Fig. 7). In the anodic sweep, the reduction process starts again after a partial desorption of the Pb-monolayer in peak D_2.

On the Ag (1 0 0) face, the reduction current decreases at the lead potential peak A_1 and vanishes after passing the peak A_2 (Fig. 8). In the anodic sweep an increase of the reduction current takes place at the lead desorption peak D_2.

Figs. 9 and 10 show the characteristic voltammograms for the thallium underpotential deposition on Ag (1 1 1) and Ag (1 0 0) faces, respectively, in the absence of NO_3^- ions as well as the influence of the Tl-adsorbates on the reduction process in the presence of NO_3^- ions in system II.

Corresponding to the effect of lead adsorption on Ag (1 1 1) (Fig. 7) the current density of the reduction process vanishes after completing the first Tl-monolayer on Ag (1 1 1) in peak A_3 (Fig. 9).

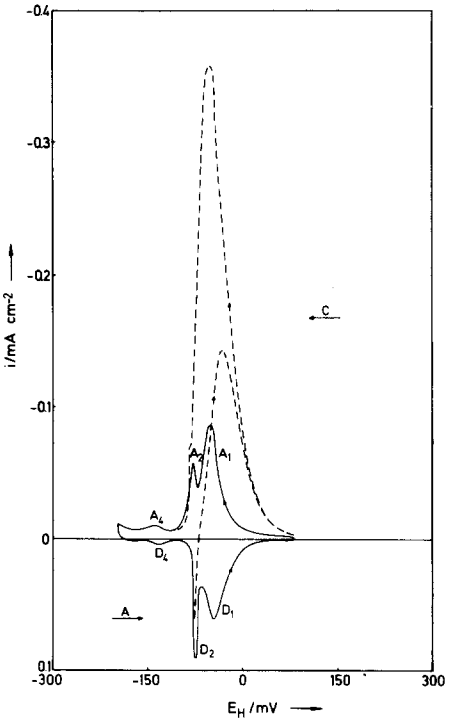

Fig. 8. System: Ag (1 0 0)/0·5 M $NaClO_4$ + 5 × 10^{-3} M $HClO_4$ + 5 × 10^{-4} M Pb $(ClO_4)_2$ + y M $NaNO_3$; (——) $y = 0$; (- - - -) $y = 0{\cdot}1$; $T = 298$ K, $|dE/dt| = 10$ mV s^{-1}, rotation frequency 25 Hz.

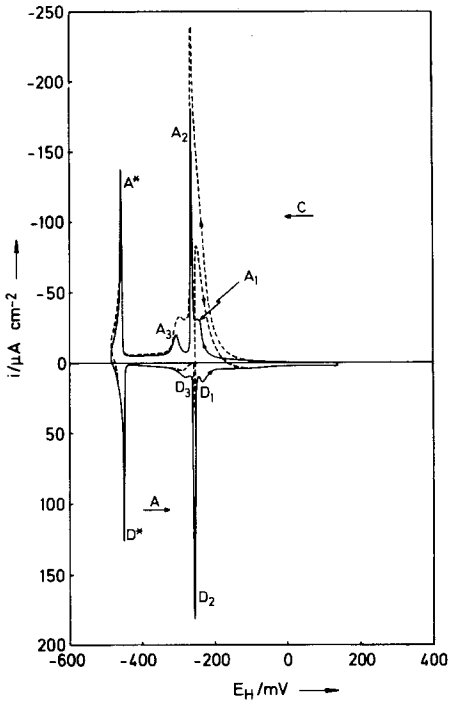

Fig. 9. System: Ag (1 1 1)/0·5 M Na_2SO_4 + 10^{-3} M $HClO_4$ + 10^{-2} M Tl_2SO_4 + y M $NaNO_3$; (——) $y = 0$; (- - - -) $y = 0{\cdot}1$; $T = 298$ K, $|dE/dt| = 10$ mV s^{-1}, rotation frequency 25 Hz.

Then, the formation of the second Tl-monolayer in peak A* is not influenced by the totally inhibited reduction process as can be seen by a comparison of the voltammograms in the absence and in the presence of NO_3^- ions in system II. Anodically, the reduction current occurs already at a partial desorption of the Tl-monolayer in peak D_3.

On the Ag (1 0 0) face a complete inhibition of the reduction process is observed after passing the peak A_2 (Fig. 10). At more negative potentials, the voltammogram of the Tl-adsorption at peak A_3 is the same as in the absence of NO_3^- ions in system II. As soon as Tl is anodically desorbed at peak D_2, the reduction reaction starts again.

A variation in the metal ion bulk concentration causes a Nernstian shift of the underpotential metal deposition range. However, it was observed that the inhibition of the reduction process is strongly correlated only to the characteristic peaks of the cyclic voltammograms of the underpotential metal deposits. This means that the degree of the surface coverage of the adsorbed metal ions deter-

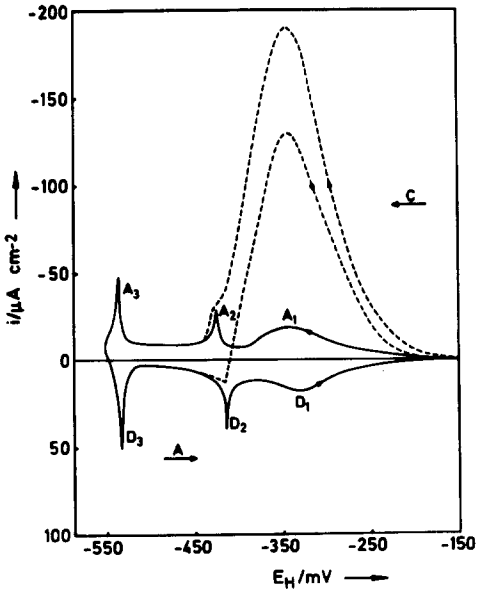

Fig. 10. System: Ag (1 0 0)/0·5 M Na_2SO_4 + 10^{-3} M $HClO_4$ + 5 × 10^{-4} M Tl_2SO_4 + y M $NaNO_3$; (——) $y = 0$; (- - - -) $y = 0{\cdot}01$; $T = 298$ K, $|dE/dt| = 10$ mV s^{-1}, rotation frequency 25 Hz.

mines the extent of the inhibition effect on the reduction process.

The reduction process on the Ag(1 1 0) face occurs at relatively negative potentials (Figs. 2 and 3). Under the experimental conditions used, the underpotential Pb- and Tl-deposits are formed at more positive potentials causing a complete inhibition effect of the reduction process. Evidently, a superposition of both processes, the reduction and the underpotential metal deposition, is only available by increasing the NO_3^- bulk concentration and by decreasing the metal ion bulk concentration, where the latter has to be changed by several orders of magnitude. However, the underpotential metal deposition process at very low metal ion bulk concentration becomes strongly diffusion controlled. In this case, an exact correlation between the degree of the metal ion coverage and the inhibition effect has not been realized experimentally.

Measurements in the systems I and II in the absence of metal ions ($y = 0$) using lead and thallium electrodes instead of silver single crystals showed a reduction current corresponding to a hydrogen evolution reaction, at very negative potentials ($E_H < -500$ mV).

4. Discussion

The results show that Pb- and Tl-coverages on Ag($h\,k\,l$) in the underpotential range do not influence the outer-sphere Fe^{3+} and Ce^{4+} reductions under limiting diffusion conditions. The limiting diffusion current density of such processes can be influenced only by a geometrical blocking effect due to an extremely high degree of coverage of indifferent and non-electronic conducting material. In this case, a decrease of the limiting diffusion current density on the rotating disc can be expected only if the mean distance between the single parts of the uncovered area (pores) becomes comparable with the thickness of the diffusion layer.

In contrast to this, a strong inhibition effect of the underpotential metal adsorbates has been found on the reduction process occurring in the presence of NO_3^- ions. Obviously, there exists a strong correlation between the inhibition effect and the surface coverage of the metal adsorbates.

In the case of the Ag(1 1 1) substrate, the reduction process is totally inhibited after the first close-packed Pb- or Tl-monolayer Ag(1 1 1)–3(2 × 2)Me in peak A_3 is formed. However, the reduction current is only reduced at lower coverages of the metal adsorbates. This can be easily interpreted by the previously assumed superlattice structures of lower density [13–16], e.g. Ag(1 1 1)–(2 × 2)Me and Ag(1 1 1)–2(2 × 2)Me, which still allow a contact between the reactant or a reaction intermediate and the Ag-substrate. The anodic sweeps of the voltammograms show that the reduction does not start before the close-packed metal adsorbate is partially desorbed.

On the Ag(1 0 0) substrate, the reduction process is totally inhibited only by the complete formation of two metal adsorbate layers corresponding to the peaks A_1 and A_2 assuming a superlattice structure Ag(1 0 0)–c(2 × 2)Me–c(2 × 2)Me [5–7, 9]. It is proposed that the second layer is situated on top of the first one filling up the uncovered adsorption sites of the silver substrate which are not occupied by the first layer. Correspondingly, a reduction current is observed in the anodic sweep as soon as the second layer is desorbed partially in peak D_2.

The observed inhibition effect of metal adsorbates on the reduction process in the presence of NO_3^- ions can be interpreted assuming a strong chemical interaction between the reactant, or a reaction intermediate and the silver substrate only. In other words, the exchange current density of the reduction process depends on the nature of the substrate.

The type of specifically adsorbed species participating in the measured reduction process is not yet clear. First of all, the observed limiting diffusion current densities (Figs. 2–6) can be attributed to a dominant proton transport process. Moreover, the charge transfer controlled reduction process cannot be unequivocally correlated with a direct discharge of NO_3^- ion as was done recently under similar experimental conditions [48]. It has been found that the charge transfer controlled part of the polarization curve is shifted to more negative potentials with decreasing NO_3^- ion concentration in the electrolyte, whereas the limiting diffusion current density remains unchanged. A reasonable assumption would be to regard the charge transfer controlled reduction

process as being caused by a rate-determining hydrogen evolution reaction. However, this process takes place on Ag($h\,k\,l$) surfaces in systems I and II in the absence of NO_3^- ions only at much more negative potentials (Figs. 5 and 6). Therefore, the charge transfer controlled process in the presence of NO_3^- ions might be ascribed to a hydrogen evolution reaction being strongly catalysed by NO_3^- ions and/or to the discharge of an intermediate within the (still unclear) NO_3^- reduction process under the experimental conditions used.

In the former case, the acceleration of the hydrogen formation requires proton donation. Specifically adsorbed NO_3^- ions as well as reduction products, e.g. NO_2^- ions or nitrogen oxide species, may act as such proton donors

$$X_{ads} + H^+ \rightleftharpoons (XH^+)_{ads} \qquad (9)$$

$$(XH^+)_{ads} + e^- \rightleftharpoons X_{ads} + H_{ads}. \qquad (10)$$

An electrocatalytic effect appears if Reaction 10 is faster than the direct discharge of protons. The well-known catalytic hydrogen waves in polarography are explained by the same effect [37].

In the latter case, the discharge of an adsorbed intermediate within the NO_3^- reduction process would require not only a valency change of the nitrogen involved in the unknown species X_{ads} but also the participation of protons in this reaction step, since the bulk diffusion of protons becomes the rate-determining step at higher overvoltages. The formation of NO_2^- ions has been observed experimentally. Therefore, either a direct discharge of adsorbed NO_3^- ions or an indirect reduction of NO_3^- ions by primarily formed H_{ads}, corresponding to Equations 7 and 8, might occur.

Experiments under hydrogen atmospheres as well as in the presence of both NO_3^- and NO_2^- ions did not show significant differences in comparison with the described behaviour. Therefore, the mechanism of the reduction process must be elucidated by further experiments. The fact remains that the reduction process is an inner-sphere reaction, which can be strongly influenced by metal adsorbates in the underpotential range as has been demonstrated.

5. Conclusions

The experimental results show that an inner-sphere redox reaction is strongly influenced by the underpotential metal adsorption on a foreign metal substrate. The definite correlation found between the metal adsorbate coverage and the degree of inhibition effect confirms the presumption that ordered metal adsorbate structures depending on the substrate orientation and on the underpotential range are formed. If the chemical interaction between the reactant and the substrate is much higher than that between the reactant and the metal adsorbate, a complete inhibition of the redox process appears as soon as the substrate is completely covered with the metal adsorbate. The assumed superlattice structures of underpotential metal adsorbates on Ag($h\,k\,l$) faces are in agreement with the experimental results.

Acknowledgements

The authors thank the Deutsche Forschungsgemeinschaft and the Fonds der Chemischen Industrie for financial support. Also the Alexander von Humboldt-Stiftung and the University of Karlsruhe are thanked for making this project possible for one of the authors (C. M.).

References

[1] W. J. Lorenz, H. D. Herrmann, N. Wüthrich and F. Hilbert, *J. Electrochem. Soc.* **121** (1974) 1167.
[2] F. Hilbert, C. Mayer and W. J. Lorenz, *J. Electroanalyt. Chem.* **47** (1973) 167.
[3] K. Jüttner, G. Staikov, W. J. Lorenz and E. Schmidt, *ibid* **80** (1977) 67.
[4] G. Staikov, K. Jüttner, W. J. Lorenz and E. Schmidt, *Electrochim. Acta* **23** (1978) 305.
[5] G. Staikov, K. Jüttner, W. J. Lorenz and E. Budevski, *ibid* **23** (1978) 319.
[6] *Idem, ibid* **90** (1978) 413.
[7] H. Bort, K. Jüttner, W. J. Lorenz and E. Schmidt, *J. Electroanalyt. Chem.*, in press.
[8] W. J. Lorenz, E. Schmidt, G. Staikov and H. Bort, 'Metal Ion Adsorption and Electrocrystallization', *Faraday Symposium No. 12*, Southampton, England (1977) to be published.
[9] H. Siegenthaler, K. Jüttner, E. Schmidt and W. J. Lorenz, *Electrochim. Acta* **23** (1978) 1009.
[10] K. Jüttner and H. Siegenthaler, *Electrochim. Acta* **23** (1978) 971.
[11] A. Bewick and B. Thomas, *J. Electroanalyt. Chem.* **65** (1975) 911.
[12] *Idem, ibid* **70** (1976) 239.
[13] *Idem, ibid* **85** (1977) 329.

[14] *Idem, ibid* **84** (1977) 127.
[15] A. Bewick, J. Jovicevic and B. Thomas, 'Phase Formation in the Underpotential Deposition of Metals', *Faraday Symposium No. 12*, Southampton, England (1977) to be published.
[16] D. Dickertmann, F. D. Koppitz and J. W. Schultze, *Electrochim. Acta* **21** (1976) 967.
[17] J. W. Schultze and F. D. Koppitz, *ibid* **21** (1976) 327.
[18] J. W. Schultze, *International Symposium Industrial Electrochemistry*, Madras, India (1976).
[19] L. Pauling, 'The Nature of the Chemical Bond', 3rd edition, Cornell University Press, Ithaca, New York (1960).
[20] R. R. Adzic and A. R. Despic, *J. Chem. Phys.* **61** (1974) 3482.
[21] R. R. Adzic, B. Z. Nikolic and A. R. Despic, 'The Effects of Foreign Metal Monolayers on the Rates of Charge Transfer Processes in Some Redox Couples', *27th ISE Meeting*, Zurich, Switzerland (1976).
[22] R. Wetzel, L. Müller and D. Majohr, *Z. Phys. Chem.* **256** (1975) 990.
[23] R. R. Adzic, D. N. Simic, A. R.Despic and D. M. Drazic, *J. Electroanalyt. Chem.* **61** (1975) 117.
[24] *Idem, ibid* **65** (1975) 587.
[25] R. R. Adzic, A. R. Despic and M. D. Spasojevic, 'Oxidation of Formic Acid on Palladium Electrode: Catalytic Effects of Foreign Metal Adatomes', *28th ISE Meeting*, Varna, Bulgaria (1977).
[26] R. R. Adzic, A. R. Despic and A. Tripkovic, 'Oxidation of Formic Acid on Rhodium Electrode: Catalytic Effects of Foreign Metal Adatomes', *28th ISE Meeting*, Varna, Bulgaria (1977).
[27] M. W. Breiter, *J. Electroanalyt. Chem.* **23** (1969) 173.
[28] M. Watanabe and S. Motoo, *ibid* **60** (1975) 259.
[29] *Idem, ibid* **60** (1975) 267.
[30] *Idem, ibid* **60** (1975) 275.
[31] R. R. Adzic and A. R. Despic, *Z. Phys. Chem. NF.* **98** (1975) 95.
[32] N. Furuya and S. Motoo, *J. Electroanalyt. Chem.* **72** (1976) 165.
[33] M. W. Breiter, *J. Electrochem. Soc.* **114** (1967) 1125.
[34] S. H. Cadle and S. Bruckenstein, *Analyt. Chem.* **43** (1971) 1858.
[35] S. N. Malischeva, O. A. Petrii and W. E. Kazarinov, *Electrokimiya* 9 (1973) 384.
[36] I. Moumtzis and W. J. Lorenz, *Chim. Chronika, N.S.* **1** (1972) 3.
[37] K. J. Vetter, 'Electrochemical Kinetics', Academic Press, New York (1967) p. 455.
[38] J. O. M. Bockris, R. J. Mannan and A. Damjanovic, *J. Chem. Phys.* **48** (1968) 1898.
[39] D. H. Angell and T. Dickinson, *J. Electroanalyt. Chem.* **35** (1972) 55.
[40] D. Galizzioli and S. Trassati, *ibid* **44** (1973) 367.
[41] M. S. Abdelaal, A. A. El Miligy, G. Reiners and W. J. Lorenz, *Electrochim. Acta* **20** (1975) 507.
[42] G. Hertz, W. J. Lorenz and G. Reiners, *Ber. Bunsenges. phys. Chem.*, submitted for publication.
[43] W. Plieth, 'Enzyclopedia of Electrochemistry of the Elements', Vol. VIII, Marcel Dekker, New York, in press.
[44] G. Schmid and M. A. Lobeck, *Ber. Bunsenges. phys. Chem.* **73** (1969) 189.
[45] G. Schmid, M. A. Lobeck and H. Keiser, *ibid* **74** (1970) 1035.
[46] *Idem, ibid* **76** (1972) 151.
[47] N. I. Alekseeva, Y. D. Zytner and V. A. Nikolskii, *Zh. Prik. Khim., Leningrad* **43** (1970) 2463.
[48] T. Vitanov and A. Popov, *Trans. SAEST* **10** (1975) 5.
[49] Y. Miyoshi and W. J. Lorenz, *Ber. Bunsenges. phys. Chem.* **74** (1970) 412.